archives
of thermodynamics
Vol. **43**(2022), No. 2, 75–96
DOI: 10.24425/ather.2022.141979

Fluid solid interactions – a novelty in industrial applications

TOMASZ OCHRYMIUK[a*]
MARIUSZ BANASZKIEWICZ[a,b]
MARCIN LEMAŃSKI[a,c]
TOMASZ KOWALCZYK[a]
PAWEŁ ZIÓŁKOWSKI[a,e]
PIOTR J. ZIÓŁKOWSKI[a]
RAFAŁ HYRZYŃSKI[a,d]
MICHAŁ STAJNKE[a]
MATEUSZ BRYK[a]
BARTOSZ KRASZEWSKI[a]
SYLWIA KRUK-GOTZMAN[a,f]
MARCIN FROISSART[a]
JANUSZ BADUR[a]

[a] Institute of Fluid Flow Machinery Polish Academy of Science, Fiszera 14, 80-331 Gdańsk, Poland

[b] General Electric Power, Stoczniowa 2, 82-300 Elbląg, Poland

[c] Anwil Grupa Orlen, Toruńska 222, 87-800 Włocławek, Poland

[d] Energa S.A. Grunwaldzka 472, 80-309 Gdańsk, Poland

[e] Gdańsk University of Technology, Narutowicza 11/12, 80-233 Gdańsk, Poland

[f] Agencja Rynku Energii, Bobrowiecka 3, 00-728 Warszawa, Poland

Abstract The article deals with a current state-of-art of fluid solid interaction (FSI) – the new branch of continuum physics. Fluid-solid interaction is a new quality of modeling physical processes of continuum mechanics, it can be described as the interaction of various (so far treated separately from the point of view of mathematical modeling) physical phenomena occurring in continuous media systems. The most correct is the simultane-

*Corresponding Author. Email: tomasz.ochrymiuk@imp.gda.pl

ous application of the laws of the given physical disciplines, which implies that fluid solid interaction is a subset of multi-physical applications where the interactions between these subsets are exchanged on the surface in interconnected systems. Our purpose is to extend the fluid solid interaction aplications into new phenomena what follow from the industrial needs and inovative thechnologies. Selecting the various approaches, we prefer the arbitraty lagrangean-eulerian description within the bulk of fluid/solid domain and a new sort of advanced boundary condition on a surface of common contact.

Keywords: Computational fluid dynamics; Computational solids dynamics; Arbitrary Lagrangian Eulerian description; Fluid solid interaction; Micro-, Nano-mechanics

1 Introduction

It was nearly 20 years ago when scientists developing the science of fluid and solid mechanics discovered that the 'flux of momentum' which is used in solid mechanics has the same nature as the 'flux of momentum' in fluid mechanics. It was indeed a revolutionary discovery that leads the army of scientists to a great novelty: if the flux of momentum within solid and fluid has the same nature then it can be exchanged on a surface of common contact, in a place where fluid touching solid body. It was a beginning of an unordinary project: to construct a science that connect CFD (computational fluid dynamics) with CSD (computational solid dynamics). The place where CFD meted CSD was a surface of solid-fluid contact, say $\mathcal{S}$. In practice, this surface is a smooth, moving, manifold oriented by unit normal vector $\mathbf{n}_s$ (from the side of solid) and $\mathbf{n}_f$ (from the side of fluid). The FSI (fluid solid interaction) it is a name of this new science.

Essentially, fluid-solid interaction opening a new perspective, it can be described as the interplay of various physical phenomena occurring in the continuum media systems with the fluid solid contact surface $\mathcal{S}$. One agrees that an impact on the system can only be registered by simultaneously applying the laws of the physical disciplines involved. Thus, generally speaking, the FSI is a subset of multi-physical applications, which typically involve a solving new kind of surface $\mathcal{S}$ boundary conditions both connected systems, governed by partial differential equations, coming from physical models of fluid and solid.

For example, thermal-FSI is the simplest, most known and popular coupling of CFD and CSD together *via* $\mathcal{S}$ and the balance of energy. It means

that the thermal coupling is described as energy transport, conversion, and exchange within a thin layer occurring in a contact with the solid and the fluid [1, 2, 11–16]. Such novelty concept need an assumption that the flux of energy in the solid body has the same nature as the flux of energy in the fluid matter. In other words, within the thermal-FSI approach, the basic assumption is that both, the solid deformation and the fluid flow, are governed by the same kind of mass, momentum conservation which should be adequately expressed for an effective fluid/solid thermal energy exchange.

Yet another applications could combine the following simulations: fluid dynamics, structure dynamics, thermal, acoustic, magnetic, electric or electromagnetic. In the biological fluid/solid systems the governing phenomena is an exchange of ions. Coupled fluid/solid systems and formulas are those that apply to multiple domains and dependent variables that typically describe different physical phenomena and in which no domain can be solved when separated from each other and no set of dependent variables can be clearly eliminated at the level of differential equations [3,5]. It is well-known that, for real industrial applications, due to their geometrical complexity, there is a pointless search for quasi-analytical or linearized solutions – it is necessary to use classical numerical techniques like CFD and CSD. Therefore, starting from CFD or CSD one can obtain a different look on FSI numerical tools. Therefore, in the literature [4,6] there are many various, sometimes inconsistent, strategies for numerical solutions FSI problems.

Only the arbitrary Lagrangian-Eulerian (ALE) description gives a proper foundation for monolithic methods in which simultaneous solution for all unknowns of the coupled fluid/solid system [7, 9, 10]: all interaction effects between the dependent equations are covered; or partitioned methods in which separate solution for the single physical fields: consideration of interaction effects by exchange of variables at the common interface $\mathcal{S}$; or finally, field elimination method eliminates of field variables at the level of differential equations. Of course, we must not forget about the most important aspect of FSI coupling, namely the physics of the phenomenon. Depending on the physical nature of the interaction different coupling methods [5–8] for the involved physical fields are required like alternating solution of solid and fluid problems with simple interchange of boundary conditions for $\mathcal{S}$ (explicit coupling); solving the equations simultaneously (implicit coupling) or combining a monolithic solver with a partitioned scheme (intermediate strategy).

In the numerical literature, the practice of FSI is dominated philosophy. Thus, from practical point of view there are three strategies [9, 10] for FSI-problems approaching. First, so-called weak coupled method (one-way) in which the information interchange between subtasks is provided only once per time step and no iteration for overall solution within time step is available. Second, strong coupled method (two-way) – iteration for overall solution within each time step gives a time accurate solution. And third one, simultaneous solution in which the subfields are solved within only one iteration using a consistent discretization in space and time.

The aim of our paper is to present a numerous achievements [11–35] of the Department of Energy Conversion Institute of Fluid Flow Machinery Polish Academy of Sciences (IMP PAN) in a quite new arrangement. Our contribution is the consistent development and application of the comprehensive FSI problem to solve specific engineering problems, with particular emphasis on the exploitation of energy devices. This allows for the development of a number of recommendations and procedures that are already commonly used in numerical modeling of complex, coupled heat-flow phenomena, where feedback occurs most often from the solid state. This computational philosophy is a relatively innovative approach and will probably successfully replace the classic modelling approach with a separated CFD and CSD. We are extending the basic assumption of FSI, that speaks on the same nature of momentum flux occurring in solid and fluid, into an extended assumption that every fluxes which appears within the fluid have the same physical nature as adequate fluxes within solid body. Therefore, by equalling these fluxes on $\mathcal{S}$ we obtain such subdomains of FSI as: mass-FSI, momentum-FSI, thermal-FSI, electrical-FSI, and so on. For instance, the angular momentum-FSI has been developed in [29], the biological-FSI in [27] (see Table 1). We have also hope, that our assumption about the physical equivalence of every fluxes, will be a 'never-ending novelty' of a corner stone for this new branch of continuum physics as is the FSI.

Table 1: Subdivision of different types of fluid solid interaction science.

Main mode of fluid/solid coupling *via*	Type of FSI
Mass balance	mass-FSI
Momentum balance	momentum-FSI
Energy balance	thermal-FSI
Electric current balance	electrical-FSI
Ions balance	biological-FSI

2 Momentum-FSI – the arbitrary Lagrangian–Eulerian form of the balance equations

The set of the ALE balance of mass, momentum and energy equations can be expressed in the following form [10]:

$$\frac{\partial}{\partial t}\begin{Bmatrix}\rho\\ \rho\mathbf{v}\\ \rho e\end{Bmatrix}+\operatorname{div}\begin{Bmatrix}\rho\mathbf{c}\\ \rho\mathbf{v}\otimes\mathbf{c}\\ \rho e\mathbf{c}\end{Bmatrix}=\operatorname{div}\begin{Bmatrix}0\\ \mathbf{t}\\ \mathbf{t}\,\mathbf{v}+\mathbf{q}\end{Bmatrix}+\begin{Bmatrix}0\\ \rho\mathbf{b}\\ \rho\mathbf{b}\cdot\mathbf{v}\end{Bmatrix}, \tag{1}$$

which, expressing the ALE relative velocity as $\mathbf{c}=\mathbf{v}-\mathbf{w}$, can be expressed further to be

$$\frac{\partial}{\partial t}\begin{Bmatrix}\rho\\ \rho\mathbf{v}\\ \rho e\end{Bmatrix}+\operatorname{div}\begin{Bmatrix}\rho(\mathbf{v}-\mathbf{w})\\ \rho\mathbf{v}\otimes(\mathbf{v}-\mathbf{w})\\ \rho e(\mathbf{v}-\mathbf{w})\end{Bmatrix}=\operatorname{div}\begin{Bmatrix}0\\ \mathbf{t}\\ \mathbf{t}\,\mathbf{v}+\mathbf{q}\end{Bmatrix}+\begin{Bmatrix}0\\ \rho\mathbf{b}\\ \rho\mathbf{b}\cdot\mathbf{v}\end{Bmatrix}, \tag{2}$$

where ρ and $\mathbf{v}$ are the density and velocity of the continuum particle, respectively, – $\mathbf{w}$ is the discretisation lattice velocity, $e=c_vT+\frac{1}{2}\mathbf{v}^2$ is total energy, c_v is specific heat at constant volume, T is temperature of the continuum particle, $\mathbf{t}$ is the momentum flux (Cauchy stress tensor), $\mathbf{q}$ is the total heat flux, $\mathbf{b}=-9.81\mathbf{e}_z$ is the gravitational acceleration. The momentum flux, according to continuum physics tradition, can be divided into an elastic (recoverable) part and a diffusive (dissipative) part:

$$\mathbf{t}=\mathbf{p}+\boldsymbol{\tau}^c, \tag{3}$$

where $\mathbf{p}$ is called an elastic momentum flux which is reversible and $\boldsymbol{\tau}^c$ is a total diffusive momentum flux which describes irreversible phenomena.

The elastic part $\mathbf{p}$ is the spherical pressure tensor in the case of liquids and gasses which cannot transfer the elastic shear stress. In the case of solids, $\mathbf{p}$ is in the full form of the elastic stress tensor

$$\mathbf{p}=\begin{cases}-p\mathbf{I}=-p\delta_{ij}\mathbf{e}_i\otimes\mathbf{e}_j & \text{– fluid,}\\ \boldsymbol{\sigma}=\sigma_{ij}\mathbf{e}_i\otimes\mathbf{e}_j & \text{– solid,}\end{cases} \tag{4}$$

where p represents a thermodynamical pressure. The minus sign in the case of a fluid is due to the fact that the elastic momentum flux is the pressure directed towards the centre of the particle and compressing the substance.

Thermodynamic pressure is constituted usually by the Carnot–Clapeyron equation $pv = RT$.

The Hooke law for isotropic, elastic bodies is usually used as a constitutive equation in the model: $\boldsymbol{\sigma} = \mathcal{L}\boldsymbol{\varepsilon} = \mathcal{L}_{ijkl}\varepsilon_{kl}\mathbf{e}_i \otimes \mathbf{e}_i$, where $\mathcal{L}$ is four-order elasticity tensor and $\boldsymbol{\varepsilon}$ the Almansi-type deformation tensor. In numerical practise, the stress and deformation tensor are represented as the vectors $\{\sigma\}$ and $\{\varepsilon\}$, thus $\mathcal{L}$ is represented by the following 6×6 matrix of Hooke's law. For isotropic solid material this matrix is the function of Young's modulus (E) and Poisson's coefficient (ν):

$$\{\sigma\} = \begin{Bmatrix} \sigma_{11} \\ \sigma_{22} \\ \sigma_{33} \\ \sigma_{12} \\ \sigma_{23} \\ \sigma_{31} \end{Bmatrix} = \frac{E}{(1-\nu)(1-2\nu)} \begin{pmatrix} 1-\nu & \nu & \nu & & & \\ \nu & 1-\nu & \nu & & & \\ \nu & \nu & 1-\nu & & & \\ & & & 1-2\nu & & \\ & & & & 1-2\nu & \\ & & & & & 1-2\nu \end{pmatrix} \begin{Bmatrix} \varepsilon_{11} \\ \varepsilon_{22} \\ \varepsilon_{33} \\ \varepsilon_{12} \\ \varepsilon_{23} \\ \varepsilon_{31} \end{Bmatrix}. \tag{5}$$

Usually $\boldsymbol{\tau}^c = 0$ in solid but within fluid the total diffusive momentum flux is defined to be a sum of different components:

$$\boldsymbol{\tau}^c = \boldsymbol{\tau} + \mathbf{R} + \mathbf{D} + \ldots, \tag{6}$$

where $\boldsymbol{\tau}$ is a viscous momentum flux, $\mathbf{R}$ is a turbulent momentum flux, $\mathbf{D}$ is a diffusion momentum flux, dots '...' represent other fluxes that have been neglected in these considerations, e.g.: the transpirational momentum flux. The viscous momentum flux is expressed by the following Stokes equation

$$\boldsymbol{\tau} = -\frac{2}{3}\mu I_{\mathbf{d}}\mathbf{I} + 2\mu\mathbf{d}, \tag{7}$$

where μ is the molecular viscosity, $I_{\mathbf{d}} = \mathbf{trd}$ is the first invariant of the strain rate, $\mathbf{d} = \frac{1}{2}(\mathbf{v} \otimes \nabla + \nabla \otimes \mathbf{v})$ is the strain rate tensor. The turbulent momentum flux $\mathbf{R}$ also known as turbulent Reynolds stress can be written, in analogy to the Newtonian fluid, as the Boussinesq closure

$$\mathbf{R} = -\frac{2}{3}\mu_t I_d\mathbf{I} + 2\mu_t\mathbf{d}, \tag{8a}$$

where μ_t is the turbulent viscosity coefficient.

The another important balance within the bulk of fluid/solid domain, that is treated with momentum balance is an additional geometrical conservation equation that is stated on the lattice velocity $\mathbf{w}$. According to Benson [7] we take the following relation as a base for determining of lattice motion:

$$\operatorname{lap}\mathbf{w} + K\mathbf{w} = 0 \quad \text{in fluid/solid domain}, \tag{8b}$$

where K is a virtual rigidity of lattice and $\operatorname{lap}(\cdot) = \operatorname{div}\{grad(\cdot)\}$. Additionally, the following boundary condition should be satisfied:

$$\mathbf{w}_{|\mathcal{S}} = \mathbf{v}_{|\mathcal{S}} \quad \text{on} \quad \mathcal{S}. \tag{8c}$$

3 Momentum FSI boundary conditions

Now, going into boundary conditions, specific for momentum-FSI, one would consider equality of flux of momentum as a primary condition which take place on a fluid-solid, moving contact surface $\mathcal{S}$. This surface is oriented by unit normal vectors $\mathbf{n}_f$ and $\mathbf{n}_s$, respectively ($\mathbf{n}_s = -\mathbf{n}_f$). If we denote by $\mathbf{t}_s$ and $\mathbf{t}_f$ the solid and fluid stress tensors, then, according to the Cauchy theorem, on the fluid-solid boundary we obtain:

$$\mathbf{t}_f\mathbf{n}_f + \mathbf{t}_s\mathbf{n}_s = 0 \quad \text{on} \quad \mathcal{S} \quad \text{(FSI)}. \tag{9}$$

It is a classical equality of boundary forces, that can be spitted on equality of normal components (like pressure) and equality of tangent component (like friction or mobility forces). Sometime, in the practice, one uses the name: 'wall stress' for tangent components, then Eq. (9) speaks about: 'equality of wall stresses'. It was Louis Navier who assumed non-typical contact between solid and fluid. In his case the solid is stress-less, $\mathbf{t}_s = 0$, and on the boundary $\mathcal{S}$ appears, from the fluid sides, not only stress tensor $\mathbf{t}_f$ but a surface resistance force $\mathbf{f}_f^{(r)}$ that is induced by a contact of two different matters. When the condition: $\mathbf{t}_f\mathbf{n}_f + \mathbf{t}_s\mathbf{n}_s = 0$ turns into more 'richness' one

$$\mathbf{t}_f\mathbf{n}_f + \mathbf{t}_s\mathbf{n}_s + \mathbf{f}_f^{(r)} = 0. \tag{10}$$

If the Cauchy stress is defined to be uncompressible, $\mathbf{t}_f = -p\mathbf{I} + 2\mu\mathbf{d}$, and the surface friction force as $\mathbf{f}_f^{(r)} = \nu\mathbf{v}(\mathbf{I} - \mathbf{n_f} \otimes \mathbf{n_f})$ then the boundary phenomena are governed by two coefficients μ and ν. The first one μ is responsible on internal friction of two fluid layers themselves (internal

viscosity) and the second one ν – is a friction coefficient between fluid and solid material (surface viscosity).

Then the Navier boundary condition says about untypical 'ending' of fluid stresses and Eq. (10) takes an explicit form:

$$\mathbf{t}_f\mathbf{n}_f + \mathbf{f}_f^{(r)} = (-p\mathbf{I} + 2\mu\mathbf{d})\,\mathbf{n_f} + \nu\mathbf{v}\,(\mathbf{I} - \mathbf{n_f}\otimes\mathbf{n_f}) = 0. \tag{11}$$

In the literature [2,12,21,25] it is known as the Navier slip condition, where the slip length is defined as $l_s = \mu/\nu$. Dimensionless coefficient of surface viscosity, or dimensionless slip length is called: the Navier number.

In more complex manner the fluid-solid contact was built by Simon Denis Poisson – who introduced some extra surface stress $\mathbf{p}_s^{(2)}$ (from solid side). Now assuming that this surface stress is an analog of three-dimensional Cauchy stress, Poisson proposed an extension of Eq. (9) to be:

$$\mathbf{t}_f\mathbf{n}_f + \mathbf{t}_s\mathbf{n}_s + \mathrm{div}_2\,\mathbf{p}_s^{(2)} = 0. \tag{12}$$

Here, in most simplest case, the surface tensor can be interpreted as surface tension of solid body $\mathbf{p}_s^{(2)} = \gamma\,\mathbf{a}$, described by γ [MPa/m] surface tension that depends on a point and the curvature of surface $\mathcal{S}$. Note that actual contact surface $\mathcal{S}$ is described by the surface metric tensor $\mathbf{a}$ (or $\mathbf{I}_2 = \mathbf{I} - \mathbf{n}\otimes\mathbf{n} = \mathbf{a}$) and the curvature tensor $\mathbf{b} = -\mathrm{grad}_2\mathbf{n}$. Invariants of curvature tensor are the mean curvature and the Gauss curvature respectively:

$$I_{1b} = \mathrm{tr}\,\mathbf{b} = b^\alpha_\alpha = b^1_1 + b^2_2 = \frac{1}{R_1} + \frac{1}{R_2}; \quad I_{2b} = \det\mathbf{b} = \frac{1}{R_1}\frac{1}{R_2}, \tag{13}$$

where R_1 and R_2 are the main values of $\mathbf{b}$. In the Poisson condition (Eq. (12)) the two-dimensional divergence is analogical to three-dimensional one, it is defined as a contraction of two-dimensional gradient: $\mathrm{div}_2(\cdot) = \mathbb{C}_{23}\,\mathrm{grad}_2(\cdot)$. Thus, two-dimensional divergence of the Poisson surface tension is

$$\mathrm{div}_2\mathbf{p}_s^{(2)} = \mathrm{grad}_2\gamma + \gamma I_{1b}\mathbf{n}_f\,. \tag{14}$$

Poisson, in opposite to Navier, assume that the solid tensor $\mathbf{t}_s$, on the boundary has normal and tangent components: $\mathbf{t}_s\mathbf{n}_s = t_{(s)ij}n_{s(j)}\mathbf{e}_i = \sigma_{(s)n}\mathbf{n}_s + \boldsymbol{\tau}_s$ [$\boldsymbol{\tau}_s\mathbf{n}_s = 0$]. However, a fluid is static one and the Cauchy tensor becomes a function only fluid pressure, $\mathbf{t}_f = -p_f\mathbf{n}_f$. Then, finally, one can express the Poisson boundary condition (Eq. (12)) as a normal and tangential parts:

$$\Big[p_f - \sigma_{(s)n} + \gamma\,I_{1b}\Big]\,\mathbf{n}_f + [\mathrm{grad}_2\gamma + \boldsymbol{\tau}_s]\,\mathbf{a} = 0. \tag{15}$$

Let us note that the normal part of this equation was known In the literature as the Young–Laplace equation for a solid surface.

We must underline also that the Poisson approach is, in any sense, 'revolutionary' one. He was able to introduce a new, independent, object into continuum physics like the 'surface stress tensor' $\mathbf{p}^{(2)}$. Only the relatively quick development of FSI was a reason for revalorization of this forgotten object. Let us assume that, in general, $\mathbf{p}^{(2)}$ should be not treated as a simple adding of fluid and solid surface properties, $\mathbf{p}_f^{(2)}$ and $\mathbf{p}_s^{(2)}$, respectively:

$$\mathbf{p}^{(2)} = \mathbf{p}_f^{(2)} \otimes \mathbf{p}_s^{(2)} \approx \mathbf{p}_f^{(2)} + \mathbf{p}_s^{(2)} \,. \tag{16}$$

Now, in generalization of Eqs. (10) and (12), one should distinguish a reasoning line 'de Buat–Navier', that was a scientific way such scientist as Stokes, Reynolds, Maxwell, Helmholtz, Piotrowski, Duhem, Rybczyński, and Smoluchowski, from the line of Poisson. This first one is a line of reasoning that is adding to FSI boundary condition many different surface forces $\mathbf{f}_{f,s}^{(r)}$; $\mathbf{f}_{f,s}^{(a)}$; $\mathbf{f}_{f,s}^{(m)}$ [19, 25, 29, 31], etc., The second one is a line of reasoning developed: Young, Poisson, Stokes, Gibbs, Duhem, Tolman, de Korteweg, and Screven, which is focused on developing a properties of the surface stress tensor $\mathbf{p}^{(2)}$ [21]. The difference between the surface forces and the surface tensor is a fundamental one. Therefore, form physical point of view, quite different physical phenomena could be described by these objects. Thus, if someone has no imagination of it, and ignores fundamental differences than, then it is loosed in mathematics. And, the historically clean way of developing of FSI, is destroyed. Even more, in 1950 Richard Tolman, proposed an original concept of linear stress tensor of Cauchy, $\mathbf{p}^{(1)}$, that make a description of FSI contact more precise and complementary.

Finally, it was Gabriel Stokes who proposed a combination of Eqs. (10) and (12) on $\mathcal{S}$:

$$\mathbf{t}_f \mathbf{n}_f + \mathbf{t}_s \mathbf{n}_s + \mathrm{div}_2 \mathbf{p}_s^{(2)} + \mathbf{f}_{f,s}^{(r)} + \mathbf{f}_{f,s}^{(a)} = 0, \tag{17}$$

where appears additional chemical-physical adhesive force $\mathbf{f}_{f,s}^{(a)} = \varpi \mathbf{n}_f$. Further, Stokes takes the tensor $\mathbf{t}_s$ as anisotropic linear elastic $\mathbf{t}_s = \mathcal{L}\boldsymbol{\varepsilon}$ and for fluid $\mathbf{t}_f = -p\mathbf{I} + 2\mu\left(\mathbf{d} - \frac{1}{3} I_{1d}\mathbf{I}\right) - \kappa I_{1d}\mathbf{I}$. Then the FSI boundary conditions for momentum have now the extended Stokes form:

$$\left[-p\mathbf{I} + 2\mu\left(\mathbf{d} - \frac{1}{3} I_{1d}\mathbf{I}\right) - \kappa I_{1d}\mathbf{I}\right]\mathbf{n}_f + [\mathcal{L}\boldsymbol{\varepsilon}]\mathbf{n}_s + \mathrm{div}_2(\gamma\,\mathbf{a}) + \nu(\mathbf{v}_f - \mathbf{v}_s) + \varpi\mathbf{n}_f = 0. \tag{18}$$

This fundamental equation, being the basic for momentum-FSI, should be always the pattern, when we starting to more precise describing of momentum exchange between two continua. For instance, Osborne Reynolds proposed in 1879 a further generalization of Stokes (Eq. (18)) in the following form:

$$\mathbf{t}_f\mathbf{n}_f + \mathbf{t}_s\mathbf{n}_s + \mathrm{div}_2(\mathbf{p}_f^{(2)} + \mathbf{p}_s^{(2)}) + \mathbf{f}_{f,s}^{(r)} + \mathbf{f}_{f,s}^{(a)} + \mathbf{f}_{f,s}^{(m)} = 0, \tag{19}$$

where there appears an additional part $\mathbf{f}_{f,s}^{(m)}$ which is called the 'mobility force'. This force is responsible for phenomena for many surface phenomena, like 'thermal transpiration' [12, 19, 26].

4 Thermal FSI – remarks

Thermal contact on $\mathcal{S}$ depends not only of the normal flow of thermal energy but also on a tangential transport of this energy. If we add, for our considerations, a surface temperature θ_2 responsible for this surface transport, than we can extend of the classical boundary FSI condition $\mathbf{q}_f^c \cdot \mathbf{n}_f + \mathbf{q}_s^c \cdot \mathbf{n}_s = 0$ into a more advanced one. Additionally, we shall consider a thermal layer (see Fig. 1) which becomes during the contact between hot fluid and cold solid continua to be described by a thin but finite layer described by two mechanisms. The first one is the Smoluchowski thermal jump, described by the thermal length jump l_T^s and l_T^f acting from the side of fluid and solids, respectively; and the second one is the overall transport of thermal energy in macroscopic vicinity of the contact layer which are described by the overall transfer coefficients α_f and α_s. Thus, taking these above motivations into account, one can propose an advanced boundary conditions of FSI in the form of thermal energy transport within the thin thermal layer dividing hot fluid and cold solid to be [1, 20]:

$$\begin{aligned}\partial_t\left(\rho_2 c_{p2}\theta_2\right) + \mathrm{div}_2\left(\rho_2 c_{p2}\theta_2\mathbf{I}_2\mathbf{v}_2\right) + \mathrm{div}_2\left(\lambda_2\,\mathrm{grad}_2\theta_2\right)\\ + \Lambda_T^f\left(T_2^f - \theta_2\right) + \Lambda_T^s\left(T_2^s - \theta_2\right) + \alpha_f\left(T_f - T_2^f\right) + \alpha_s\left(T_s - T_2^s\right)\\ + \left(\mathbf{f}_{mech}^f \cdot \mathbf{v}_{\mathrm{slip}}^f + \mathbf{f}_{\mathrm{mech}}^{\mathbf{s}} \cdot \mathbf{v}_{\mathrm{slip}}^s\right) + \mathbf{q}_f^c \cdot \mathbf{n}_f + \mathbf{q}_s^c \cdot \mathbf{n}_s = 0.\end{aligned} \tag{20}$$

In the above equation ρ_2, c_{p2} are a mass density and heat capacity of the thermal layer, $\mathbf{v}_2$ is the velocity of thermal layer, that usually can be equal to $\mathbf{v}_{slip}^f$, λ_2 – thermal conductivity coefficient of thermal layer; $\Lambda_T^f = l_T^f/\lambda_f$ and $\Lambda_T^s = l_T^s/\lambda_s$ are the Smoluchowski jump coefficients from the fluid

and solid side, respectively; $\left(T_2^f - \theta_2\right)$ and $(T_2^s - \theta_2)$ are the Smoluchowski jump of temperature field; $\left(T_f - T_2^f\right)$ and $(T_s - T_2^s)$ are the classical transfer deriving temperatures between far-field T_s (solid) and T_f (fluid). The mechanical source of surface energy is described by surface force working on the slip velocity. And finally, in Eq. (20), the classical thermal-FSI condition, $\mathbf{q}_f^c \cdot \mathbf{n}_f + \mathbf{q}_s^c \cdot \mathbf{n}_s = 0$, describes a normal flow of thermal energy, where the total fluxes of heat, usually, are treated to be related with: diffusional (Fourierian) transport, turbulent transport, radiative, diffusional mass transport, non-elastic transport and so on:

$$\mathbf{q}_f^c = \mathbf{q}_f + \mathbf{q}_f^{\text{tur}} + \mathbf{q}_f^{\text{rad}} + \mathbf{q}_f^{\text{diff}} + \ldots \text{ (fluid)}, \tag{21}$$

$$\mathbf{q}_s^c = \mathbf{q}_s + \mathbf{q}_s^{\text{tur}} + \mathbf{q}_s^{\text{rad}} + \mathbf{q}_s^{\text{non-e}} + \ldots \text{ (solid)}. \tag{22}$$

In the above Eq. (21) and Eq. (22) most basic are still the Fourierian mode of transport described by a classical linear function of temperature gradient:

$$\mathbf{q}_s = \lambda_s \operatorname{grad} T_s; \qquad \mathbf{q}_f = \lambda_f \operatorname{grad} T_f. \tag{23}$$

Note that in the classical thermal-FSI approach, what is nothing else as 'first order approximation', there is no the Smoluchowski thermal jump, therefore fluid and solid temperatures in the thermal layer coincidences: $T_2^s = T_2^f$. If additionally we omit the surface transport of thermal energy due to overall transport ($\alpha_s = \alpha_f = 0$) we obtain: $\mathbf{q}_f^c \cdot \mathbf{n}_f + \mathbf{q}_s^c \cdot \mathbf{n}_s = 0$. But in the case of CSD, when fluid temperature is assumed to be known Eq. (20) reduce to $\alpha_f (T_f - T_s) + \mathbf{q}_s^c \cdot \mathbf{n}_s = 0$, and *vice versa*, in the case of CFD, when the solid temperature is assumed to be known Eq. (20) reduce to $\alpha_s (T_s - T_f) + \mathbf{q}_f^c \cdot \mathbf{n}_f = 0$. Dimensionless coefficients α_s and α_f are known, in the literature, as the Stanton and Biot numbers, respectively. Note that from the numerical point of view, Eq. (20) is very challenging. Additionally, at the moment, a state of the art thermal-FSI has no possibilities for numerical solution of the full energy balance within the thermal contact layer [16, 17]. The first reason of that is the insufficient development of the finite element method as well as of the finite volume method [3, 4]. Actually, both methods are prepared only in order to solve simultaneously only one part of the equation in the following classical form: $\mathbf{q}_f^c \cdot \mathbf{n}_f + \mathbf{q}_s^c \cdot \mathbf{n}_s = 0$ [14, 15, 22–24].

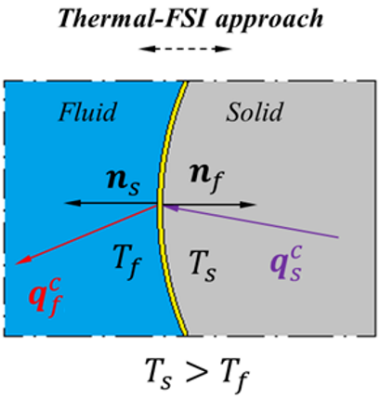

Figure 1: Realization of thermal-FSI by coupling of energy balance within the thermal contact layer, where: $\mathbf{q}_s^c$ – total diffusive heat flux in the solid body; $\mathbf{q}_f^c$ – total diffusive heat flux in the fluid/solid domain; T_s – solid temperature; T_s – fluid temperature; $\mathbf{n}$ – normal vector.

5 Mass-FSI – some remarks

When one has to describe such phenomena as 'draying of wet wood' or 'the evolution of stress-corrosion due to oxygen transport', there is a need to start with a FSI-question of coupling of fields through the balance of mass. The exchanging of mass fluxes, when we are omitting a possibility of surface mass transport, leads to the classical mass-FSI boundary condition

$$\mathbf{j}_s \cdot \mathbf{n}_s + \mathbf{j}_f \cdot \mathbf{n}_f = 0, \tag{24}$$

where the mass fluxes are described, for instance, by the isotropic Fick relations: $\mathbf{j}_f = D_f \operatorname{grad} c_f$; $\mathbf{j}_f = D_f \operatorname{grad} c_f$, where c_f and c_s are the concentration of the same species in fluid and solid, respectively. If the surface motion of species are important, then one would repeat a line of reasoning of the advanced thermal-FSI from Section 4. Especially, within a micro-flows, the surface transport of mass with the slip velocity can give particular effects [21, 28].

6 Electrical-FSI – additional remarks

Transport of electricity within the Solid Oxide Full Cells domain takes place mainly on a surface of a contact between an electrolyte and anode or between an electrolyte and cathode [21]. It is therefore some need to

develop a advanced mode of surface electric current flow. Then the classical boundary condition $\mathbf{j} \cdot \mathbf{n} = 0$ with the Ohm law $\mathbf{j} = \sigma \operatorname{grad} \phi$ one can to allow some enhancement of electric current flow due to surface flow of it:

$$\operatorname{div}_2 (\sigma_2 \operatorname{grad}_2 \phi_2) + \mathbf{j} \cdot \mathbf{n} = 0, \tag{25}$$

where the surface electric potential ϕ_2 and the surface conductivity σ_2 are possible to determine from a benchmark so-called 'triple-junction' experiment [21, 28].

7 Thermal-FSI examples

The main specialization of the Department of Energy Conversion IMP PAN is the thermal-FSI, therefore, one can find, in the literature numerous examples of our activity [2, 12, 14, 18, 30, 31, 37, 38]. Few of them are devoted to concrete, real structures as appears in industrial applications, where the thermal energy exchange is a leading phenomenon.

Let us start from the first group of examples deals with extremely 'fast start up' of different devices of power plants. The first example of thermal-FSI application is the main valve in a turbine of 400 MW (Fig. 2).

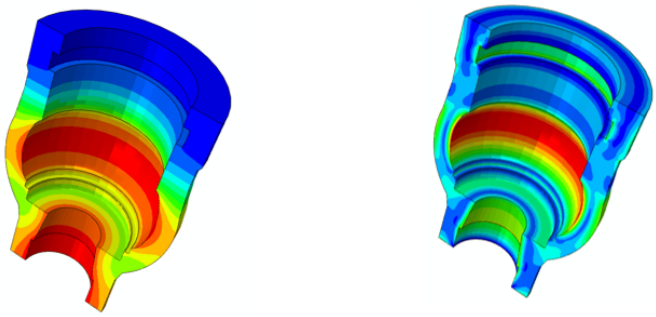

Figure 2: The distribution of temperature (left) and the Huber thermal effort in 10 min of the cold start up of the valve [35].

In that case of 'cold start-up' the rate of heating of a casing massive body has a great influence on a state of thermal stresses which we call: the 'thermal effort'. Up to now, in the literature, there is no enough attention devoted to a problem of proper describing of the phenomena [15, 18, 32], therefore we are developing researchers on an application of two concepts of thermal effort: the Huber and the Burzyński ones.

Yet another example of immediate start-up is a case of a braking cold glasses during preparation of tee, when start-up is limited to a few seconds (Figs. 3–5). In the case when a glass has a thin bottom and relatively thick walls the process of heating starting from thin plate of bottom, and due to its thermal expansion arise a great axi-symmetrical pressing of yet cold vertical wall. It leads, finally, to breaking of the glass *via* vertical (not horizontal) cracking of walls. The effective Huber-Mises-Hencky stress and the effective Burzyński stress, calculated according to the Huber and Burzyński thermal effort hypothesis, significantly differ between them, indicating that the question of 'effort hypothesis' in the case of thermal state of stresses should be stated from the very beginning.

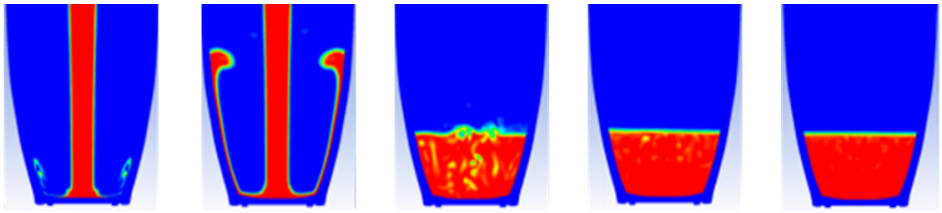

Figure 3: Distribiuton of boiling water during 3 s [13, 17].

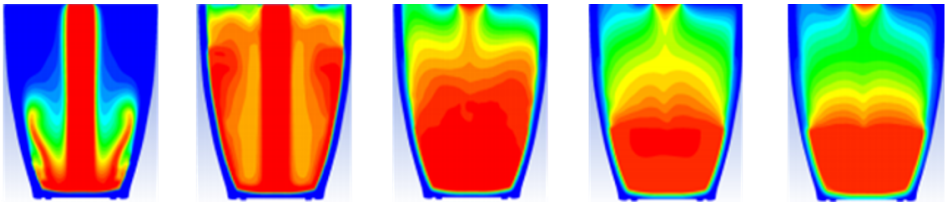

Figure 4: Temperature distribution in the water and glass body [13, 17].

The second group of thermal-FSI problems deals with cooling of hot elements of turbines and boilers during shout out. Due to enhanced flexibility of power plants there is the need for new arrangement of 'immediate shout out' of steam turbines. In Fig. 6 it is show a case of 'flooding' of working hot turbine by a very cold water, such a situation has taken place during the flooding of river Odra when some auxiliary turbine was accidentally stopped. From thermal-FSI it follows that 'immediate shout out' by cold water leads to equalization of temperatures yet after half of hour. The maximum thermal stresses appears within the rotor narrowing, and are ranges of $0.3R_m$.

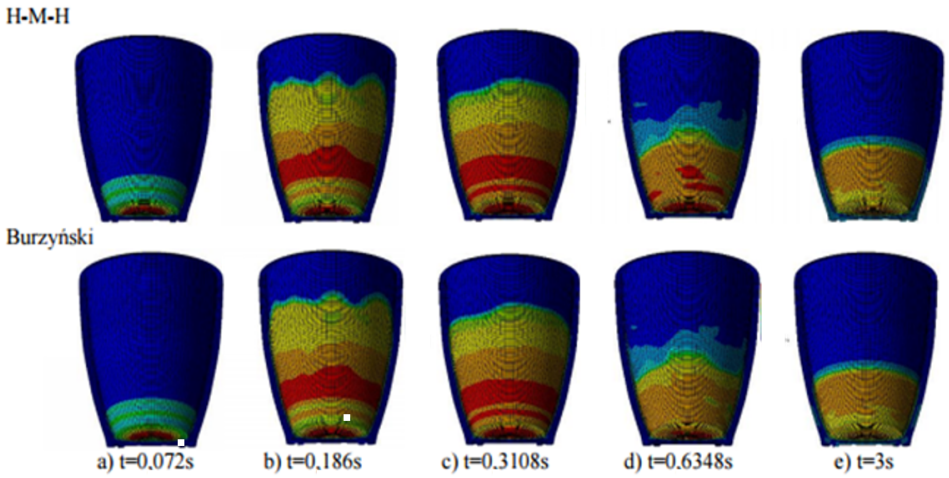

Figure 5: Distribution of the Huber and Burzyński thermal efforts during of glass heating [13, 17].

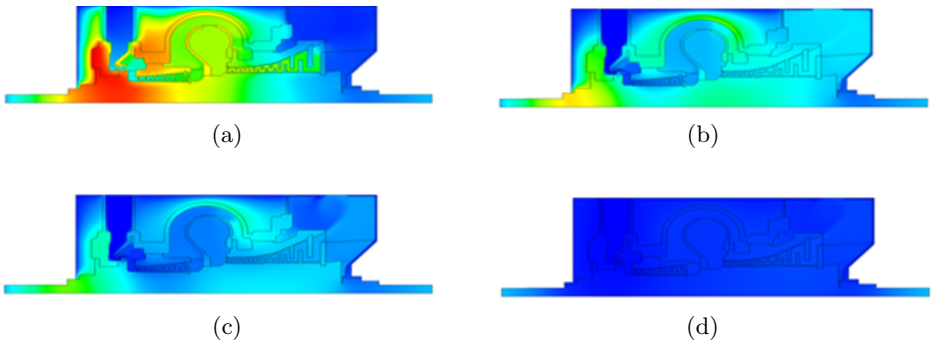

Figure 6: The temperature field of water and turbine structure metal: a) at the beginning, b) 1 h, c) 2 h, d) 12 h [16].

An another problem which appear during cooling of hot machines with rotating parts, is so-called 'wear off' of moving elements with, for instance, the casing of turbine [30,34]. Since the body of construction are usually massive and cannot shrink up in the same time as the rotor shrinking, then after few minutes of cooling the phenomena of 'wear off' starts lading to intensive vibrations and noise. In Fig. 7 it is shown of relative thermal displacements of crucial rotor elements, which indicate how huge axial clearances must be designed.

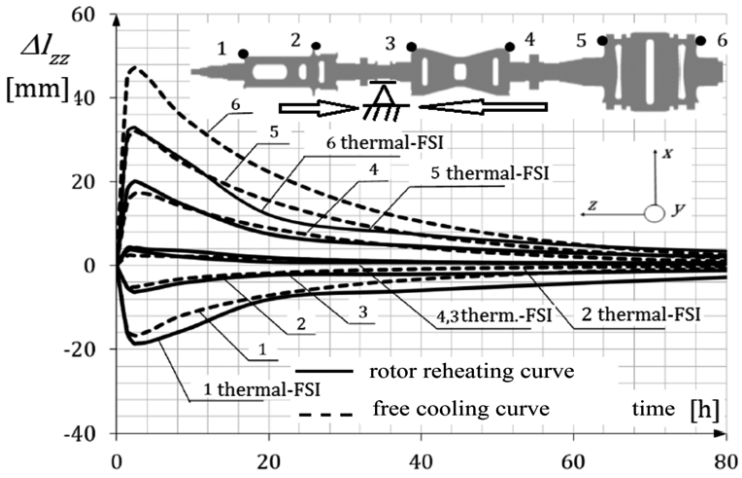

Figure 7: Comparison of thermal elongations during free and forced cooling of the 400 MW turbine rotor [30].

8 Mass-FSI examples

Stress-corrosion cracking (SCC), appearing within he blade system anchorage, is a very dangerous, delayed, failure process where corrosion is stimulated by the level of stresses. It means, cracks initiate and propagate at a slow rate (for example, 10 μm/s to 10 m/s) until the stresses, in the remaining ligament of metal, exceed the fracture strength. Since a sequence of events involved in the stress-corrosion cracking process usually consists in three stages, one can take only the main mechanism like: crack initiation, steady-state crack propagation; and crack propagation or final failure. In the case under consideration we are interested in a metal embrittlement due to the rate of corrosion, since a mode of final failure of blade was not a brittle fracture but continuous ductile, high cyclic, damage. It was assumed that a mechanism of hydrogen reaction, evolution, absorption, diffusion leads to 'embrittlement', and the front of 'embrittlement', propagate into the body, being constant within every finite element. However, this specific mechanism is able to explain the continual crack-propagation rates. The mass-FSI can provide the hydrogen of steam from internal channels of anchorage to the FSI-surface $\mathcal{S}$ where take place of adsorption of environmental species connected with surface reactions, that rates depends on the level of surface stresses. This manner of mass-FSI action can be described as: 'one-way coupling' (Fig. 8).

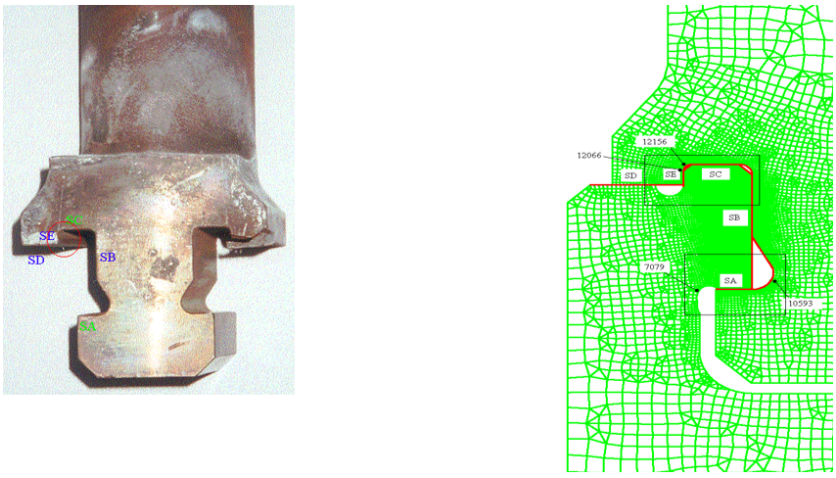

Figure 8: The domain of stress-corrosion phenomena under FEM modelling, the main surface of contact is SA-SE: SC – surface contact, SE – surface erosion, SD – surface distance, SA – surface active, SB – surface boundary; the numerical values given in the figure on the right are stresses in MPa.

For this illustration, an internal hydrogen embrittlement mechanism is assumed in order to minimize the number of possible rate-determining steps. For the typical steam turbine conditions (temperature, pressure, pH, solute concentration and activity) we have modeled surface influx of hydrogen mass, and propagation of front of embrittlement into a metal. There is the stress controlled process than the corrosion is more intensive if the stretched stresses are higher (Fig. 9). Our numerical simulation have shown

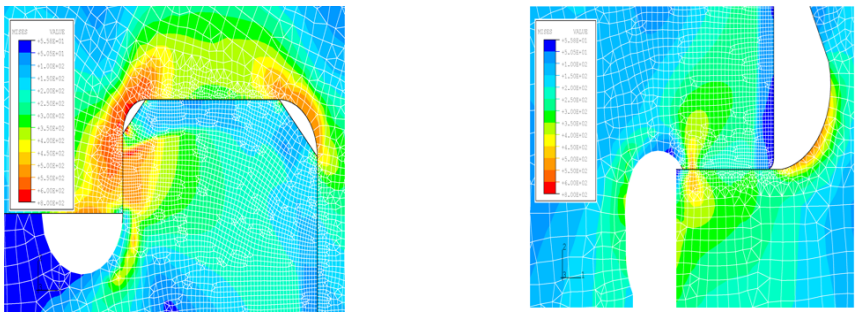

Figure 9: Resulting stresses within the corrosive layer of thickness 60 μm, the blade still under kinetic-static loading (3000 rpm) equivalent to normal blade stresses $\boldsymbol{\sigma}_{zz} = 140$ MPa.

that changes in the steam environment of 'blade food' that modify the rate-determining step will have a dramatic influence on the rate of embrittlement front propagation, while alterations to factors not involved in the rate-determining step will have little influence, if any. The observed *in situ* corrosive layer thickness 60 μm can be obtained even in the time of three weeks. It is time identical with the time of breakdown of blade.

9 Biological-FSI example

The most important are the cases of 'double-way coupling' when, due to significant displacement of solid, the motion and velocity of a moving discretization lattice **w** should be also determined. One important case is the motion of a common carotid artery (CCA), due to blood pressure pulsation during a period of 1 s. The internal diameter of the artery [normal, healthy patient] change during the period from 2.5 mm to 4.7 mm, since thin wall of the intima-media has an even negligible rigidity and is very extensible. In this case the momentum FSI boundary conditions (Eq. (19)) reduce to the so-called Young condition:

$$\tau_{\text{wall}}^{\text{intima}-\text{media}} = \tau_{\text{wall}}^{\text{blood}} < 150 \text{ Pa}, \tag{26}$$

which is known in the medicine of hypertension disease [27]. In the hypertension disease the 'wall stress' is a criterion of an illness, and the level of 150 Pa is treated to be safety for a man.

10 Momentum-FSI examples

Yet another interesting case of application of ALE description is a vibrating motion of elastic flexible steel sheet having displacements reaching even 50 time more than its thickness (see Fig. 10). It means that the 'geometrically non-linear-CSD' analysis is unalienable and the deformations of discretization lattice within the fluid domain are meaningful and cannot be ignored [10].

Going into another example, in industral practice is known a cases of a flutter motion apperaing in the last stages of turbine blades. This case needs the forced vibriation analsis, that occoears in unstationary flow of water steam within low pressure conditions. In Fig. 11 it is shown an vibrating modes induced by 'one-way coupling' simulation of the Baumann blade which occours in flutter motion with the resonance freqency $H_7 = 4300$ Hz.

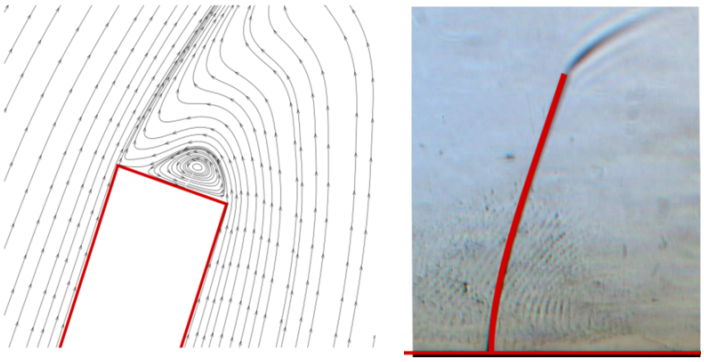

Figure 10: Motion of flexible sheet in the wind channel: a) a detail of a mode of fluid motion at the tip of sheet, b) comparison of the calculated and measurement shape of sheet [10].

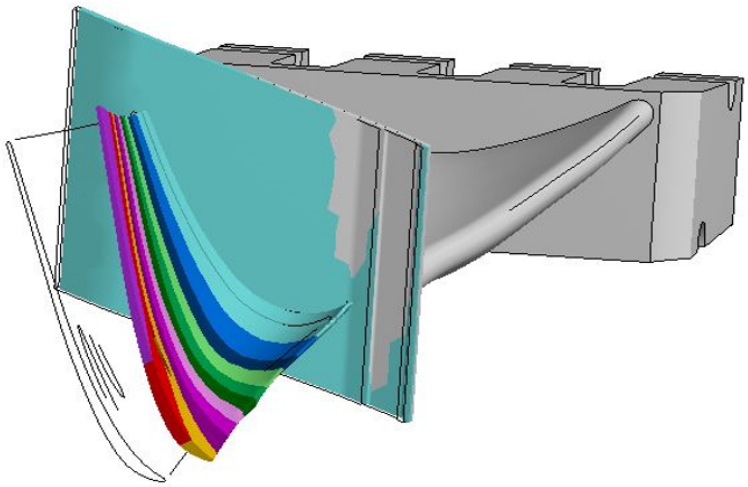

Figure 11: Resonance modes of flatter motion of the Baumann blade.

11 Conclusions

The aim of our paper is two-fold. Firstly, we want to turn an attention of reader into a possibility of incorporating a quite new range of the physical 'surface dominated phenomena' into scientific considerations. In our opinion, the fluid solid interaction (FSI) as a young science, has a very promising perspectives of developing, both within the framework of the finite volume method as well as the finite element method. It is obvious

that the 'advanced-FSI' boundary conditions governed by Eqs. (19)–(20), (24)–(25) are especially promising for description and modelling of micro- and nano-mechanics. It follows from our achievements [1,13,20,33–38] that such sophisticate phenomena like 'thermal transpiration'; or the Smoluchowski jump, can be correctly described within the framework of continuum physics [19,25].

Secondly, it was even more evident to shown the importance of numerous applications of FSI into power plant industry. In the last ten years the team of Department of Energy Conversion IFFM PAS at Gdańsk make a numerous works owing to step by step developing experience in using and developing of the FSI analytical and numerical tools. We are sure, that the numbers of application of FSI will increase sufficiently, and the 'fluid solid interaction' becomes an accepted branch of science.

Received 25 October 2021

References

[1] Badur J., Ziółkowski P., Zakrzewski W., Sławiński D., Kornet S., Kowalczyk T., Hernet T., Piotrowski R., Felincjancik J., Ziółkowski P.J.: *An advanced thermal-FSI approach to flow heating/coolin*. J. Phys. Conf. Ser. **530**(2014), 340–370.

[2] Kornet S., Ziółkowski P., Jóźwik P., Ziółkowski P., Stajnke M., Badur J.: *Thermal-FSI modeling of flow and heat transfer in a heat exchanger based on minichanels*. J. Power Technol. **97**(2017), 5, 373–381.

[3] Zienkiewicz O.C., Taylor R.L.: *The Finite Element Method*: Vol. 1 (5th Edn.). Butterworth-Heinemann, Oxford, 2000.

[4] Schäfer M., Sieber G., Sieber R., Teschauer I.: *Coupled fluid-solid problems: Examples and reliable numerical simulation*. In: Trends in Computational Structural Mechanics (W.A. Wall, Ed.), CIMNE, Barcelona 2001, 654–692.

[5] Axisa F.: *Modelling of Mechanical Systems – Fluid-Structure Interaction*. Elsevier, Berlin 2007.

[6] Bazilevs Y., Takizawa K., Tezduyar T.E.: *Computational Fluid-Structure Interaction: Methods and Applications*. John Wiley & Sons, 2013.

[7] Benson D.J., Souli M.: *Arbitrary Lagrangian Eulerian and Fluid-Structure Interaction: Numerical Simulation*. Springer-Verlag, 2010.

[8] Bodnar T., Galdi G.P., Necasova S.: *Fluid-Structure Interaction and Biomedical Applications*. Springer-Verlag, 2014.

[9] Peric D., Dettmer W.G.: *A computational strategy for interaction of fluid flow with spatial structures*. In: Proc. 5th Int. Conf. on Computational of Shell and Spatial Structures, IASS-IACM, Bochum, 2005.

[10] Ziółkowski P.J., Ochrymiuk T., Eremyev V.: Cont. Mech. Termodyn. **33**(2021), 2301–2314.

[11] Ziółkowski P., Badur J.: *A theoretical, numerical and experimental verification of the Reynolds thermal transpiration law*. Int. J. Numer. Meth. for Heat Fluid Fl. **28**(2018), 454–480.

[12] Ziółkowski P, Badur J., Ziółkowski P.J.: *An energetic analysis of a gas turbine with regenerative heating using turbine extraction at intermediate pressure-Brayton cycle advanced according to Szewalski's idea*. Energy **185**(2019), 763–786.

[13] Badur J., Ziółkowski P., Kornet S., Kowalczyk T., Banaś K., Bryk M., Ziółkowski P.J., Stajnke M.: *Enhanced energy conversion as a result of fluid-solid interaction in micro-and nanoscale*. J. Theor. Appl. Mech. **56**(2018), 1, 329–332.

[14] Kowalczyk T, Badur J., Bryk M.: *Energy and exergy analysis of hydrogen production combined with electric energy generation in a nuclear cogeneration cycle*. Energ. Convers. Manage. **198**(2019), 203–224.

[15] Badur J., Bryk M.: *Accelerated start-up of the steam turbine by means of controlled cooling steam injection*. Energy **184**(2019), 334–356.

[16] Bryk M., Kowalczyk T., Ziółkowski P., Badur J.: *The thermal effort during marine steam turbine flooding with water*. AIP Conf. Proc. **2077**(2019), 1, 020009.

[17] Kraszewski B., Bzymek G., Ziółkowski P., Badur J.: *Extremal thermal loading of a bifurcation pipe*. AIP Conf. Proc. **2077**(2019), 1, 020030.

[18] Dudda W., Banaszkiewicz M., Ziółkowski P.J.: *Validation plastic model with hardening of St12t*. AIP Conf. Proc. **2077**(2019), 020016.

[19] Szwaba R., Ochrymiuk T., Lewandowski T., Czerwinska J.: *Experimental investigation of microscale effects in perforated plate aerodynamics*. J. Fluids Eng. **135**(2013), 12.

[20] Badur J., Ziółkowski P., Kowalczyk T., Ziółkowski P.J., Stajnke M., Bryk M., Kraszewski B.: In: Proc. 6th Conf.e on Nano- and Micromechanics, Rzeszów, 3–7 July 2019.

[21] Badur J., Karcz M., Lemański M., Nastałek L.: *Enhancement Transport Phenomena in the Navier-Stokes Shell-like Slip Layer*. Computer Model. Eng. Sci. **73**(2011), 299–310.

[22] Banaś K., Badur J.: *Influence of strength differential effect on material effort of a turbine guide vane based on thermoelastoplastic analysis*. J. Therm. Stress. **40**(2017), 1368–1385.

[23] Kornet S., Badur J.: *Infuence of turbulence RANS models on heat transfer coefficients and stress distribution during thermal-FSI analysis of power turbine guide vane of helicopter turbine engine PZL-10W taking into account convergence of heat flux*. Prog. Comput. Fluid Dyn. **17**(2017), 352–360.

[24] Ziółkowski P., Kowalczyk T., Kornet S., Badur J.: *On low-grade waste heat utilization from a supercritical steam power plant using an ORC-bottoming cycle coupled with two sources of heat*. Energ. Convers. Manage. **146**(2017), 158–173.

[25] Ziółkowski P., Badur J.: *On Navier slip and Reynolds transpiration numbers*. Arch. Mech. **70**(2018), 269–300.

[26] Ziółkowski P., Badur J.: *Navier number and transition to turbulence*. J. Phys. Conf. Ser. **530**(2014), 1–8.

[27] Czechowicz K, Badur J, Narkiewicz K.: *Two-way FSI modelling of blood flow through CCA accounting on-line medical diagnostics in hypertension*. J. Phys. Conf. Ser. **530**(2014), 1–8.

[28] Badur J., Lemański M., Kowalczyk T., Ziółkowski P., Kornet P.: *Zero-dimensional robust model of an SOFC with internal reforming for hybrid energy cycles*. Energy **158**(2018), 128–138.

[29] Badur J., Ziółkowski P.J., Ziółkowski P.: *On the angular velocity slip in nano-flows*. Microfluid Nanofluid **19**(2015), 191–198.

[30] Badur J., Ziółkowski P., Sławiński D., Kornet S.: *An approach for estimation of water wall degradation within pulverized-coal boilers*. Energy **92**(2015), 142–152.

[31] Felicjancik J., Ziółkowski P., Badur J.: *An advanced thermal-FSI approach of an evaporation of air heat pump*. Trans. Inst. Fluid-Flow Mach. **129**(2015), 111–141.

[32] Badur J., Stajnke M., Ziółkowski P., Jóźwik P., Bojar Z., Ziółkowski P.J.: *Mathematical modeling of hydrogen production performance in thermocatalytic reactor based on the intermetallic phase of Ni3Al*. Arch. Thermodyn. **3**(2019), 3–26.

[33] Badur J., Ziółkowski P., Kornet S., Stajnke M., Bryk M., Banaś K., Ziółkowski P.J.: *The effort of the steam turbine caused by a flood wave load*. AIP Conf. Proc. **1822**(2017), 1, 020001.

[34] Badur J., Bryk M., Ziółkowski P., Sławiński D., Ziółkowski P.J., Kornet S., Stajnke M.: *On a comparison of Huber–Mises–Hencky with Burzynski-Pecherski equivalent stresses for glass body during nonstationary thermal load*. AIP Conf. Proc. **1822**(2017), 1, 020002.

[35] Banaszkiewicz M.: *On-line monitoring and control of thermal stresses in steam turbine rotors*. Appl. Therm. Eng. **94**(2016), 763–776

[36] Ochrymiuk T.: *Numerical analysis of microholes film/effusion cooling effectiveness*. J. Therm. Sci. **26**(2017), 5, 459–464.

[37] Ochrymiuk T.: *Numerical prediction of film cooling effectiveness over flat plate using variable turbulent Prandtl number closures*. J. Therm. Sci. **25**(2016), 3, 280–286.

[38] Ochrymiuk T.: *Numerical investigations of the 3D transonic field and heat transfer at the over-tip casing in a HP-turbine stage*. Appl. Therm. Eng. **103**(2016), 411–418.

[39] Froissart M., Ziolkowski P., Dudda W., Badur J.: *Heat exchange enhancement of jet impingement cooling with the novel humped-cone heat sink*. Case Stud. Therm. Eng. **28**(2021), 1, 101445101445.